Int. J. Heat Mass Transfer. Vol. 24, pp. 109–116
Pergamon Press Ltd. 1981. Printed in Great Britain

0017-9310/81/0101-0109 $02.00/0

GENERAL FEATURES OF CHF OF FORCED CONVECTION BOILING IN VERTICAL CONCENTRIC ANNULI WITH A UNIFORMLY HEATED ROD AND ZERO INLET SUBCOOLING

Y. KATTO
Department of Mechanical Engineering, University of Tokyo,
Hongo, Bunkyo-ky, Tokyo, Japan

(*Received* 18 *January* 1980)

Abstract—A graphical method is employed to give a generalized bird's-eye view of the existing data for critical heat flux (CHF) in internally and uniformly heated vertical annuli with zero inlet subcooling. 301 data points collected from 25 sources are used for this purpose, including 7 different fluids (water, R-12, R-114, acetone, toluene, monoisopropyl-biphenyl, and sodium), axial length of heated rod from 0.0762 to 8.84 m, outer diameter of heated rod from 0.00500 to 0.0964 m, inner diameter of unheated shroud tube from 0.0127 to 0.101 m, and vapor/liquid density ratio from 0.0000580 to 0.160.

NOMENCLATURE

d_{he}, heated equivalent diameter [m], equation (3) for inside uniform heating;
d_i, O.D. of heated rod [m];
d_o, I.D. of unheated shroud tube [m];
G, mass velocity [kgm^{-2} s^{-1}];
H_{fg}, latent heat of evaporation [Jkg^{-1}];
ΔH_i, enthalpy of inlet subcooling [Jkg^{-1}];
l, axial length of heated rod [m];
p, absolute pressure [bar];
q_c, critical heat flux [Wm^{-2}];
q_{co}, q_c for $\Delta H_i = 0$ [Wm^{-2}];
ΔT_i, inlet subcooling temperature [°C].

Greek symbols

ρ_l, density of liquid [kgm^{-3}];
ρ_v, density of vapor [kgm^{-3}];
σ, surface tension [Nm^{-1}];
χ, quality (χ_{ex}: exit quality, χ_{in}: inlet quality).

1. INTRODUCTION

RECENTLY, the author made studies [1–3] of generalized correlation equations for critical heat flux (CHF) of forced convection boiling in uniformly heated vertical tubes, and it was followed by a study [4] in which a graphical method was evolved to give a generalized bird's-eye view of the existing data of CHF in case of zero inlet subcooling.

On the other hand, existing data of CHF in uniformly heated vertical annuli were also analyzed by the author [5], revealing that the data of CHF in annuli with inside heating are correlated by a set of proper correlation equations, while CHF in annuli with outside heating can be correlated by making use of the above-mentioned correlation equations of CHF in vertical tubes. Then, following the similar way as in the case of tubes, an additional study is attempted in the present paper to give a generalized graphic representation of the existing data of CHF in internally heated annuli with zero inlet subcooling.†

2. COLLECTION OF q_{co} DATA

2.1. *Method of obtaining* q_{co} *data*

From the sources [6–31] listed in Table 1, the data of q_{co} are obtained for pulsation-free upflow, mostly by the following normal methods (i) and (ii), and for the rest, by two exceptional methods (iii) and (iv).

(i) As for the data-source providing the variation of q_c with ΔH_i (or ΔT_i, χ_{in} etc.) for fixed G such as shown in Figs 1 and 2, if there are enough data points up to the vicinity of $\Delta H_i = 0$, q_{co} can be estimated by the extrapolation as ΔH_i (or ΔT_i, χ_{in} etc.) $\rightarrow 0$. Knoebel *et al.* [19], who presented the data of q_c including those of Fig. 2, gave the following empirical equation to correlate their data of q_c in the range of $\Delta T_i > 25$°C (that is, excluding data below 25°C subcooling from the correlation):

$$q_c[\mathrm{Wm^{-2}}] = 4.844 \times 10^5(1 + 0.169V[\mathrm{ms^{-1}}])(1 + 0.12\Delta T_i[°\mathrm{C}]) \quad (1)$$

where V is the inlet velocity of water; and the broken line shown in Fig. 2 represents equation (1). However, the author's correlation of CHF of forced convection boiling (cf. [1, 2] for tubes and [5] for annuli) regards the result of Fig. 2 only as belonging to a characteristic regime called N-regime, which is distinguished by non-linear q_c–ΔH_i relationship, and q_{co} is determined by the conventional extrapolation as $\Delta T_i \rightarrow 0$ in Fig. 2.

(ii) As for the data-source providing the variation of q_c with χ_{ex} for fixed G, the relation of q_c vs ΔH_i can be derived from the following heat balance equation for

† The effect of inlet subcooling on CHF can be estimated theoretically in the same way as that shown for CHF in vertical tubes [3], so that the discussion on the effect of inlet subcooling is omitted.

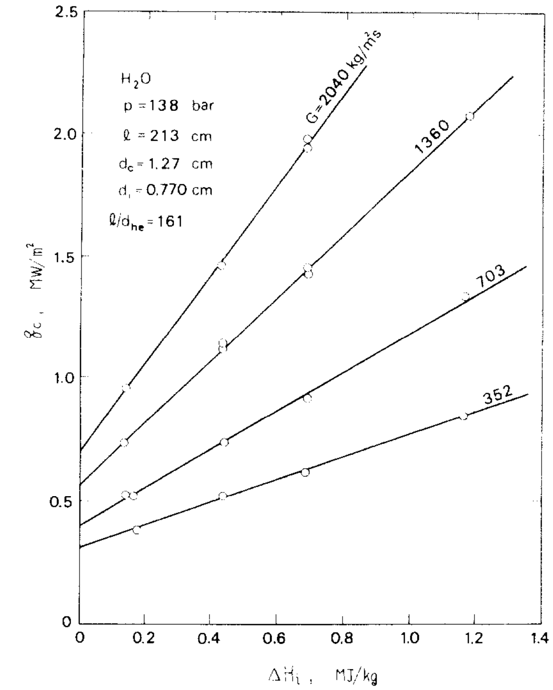

FIG. 1. Examples of the linear relationship between q_c and ΔH_i (data from Table A of Mortimore and Beus [25]).

uniformly heated annuli:

$$\frac{4q_c}{GH_{fg}} \cdot \frac{l}{d_{he}} - \frac{\Delta H_i}{H_{fg}} = \chi_{ex} \tag{2}$$

where d_{he}, the heated equivalent diameter, is given for

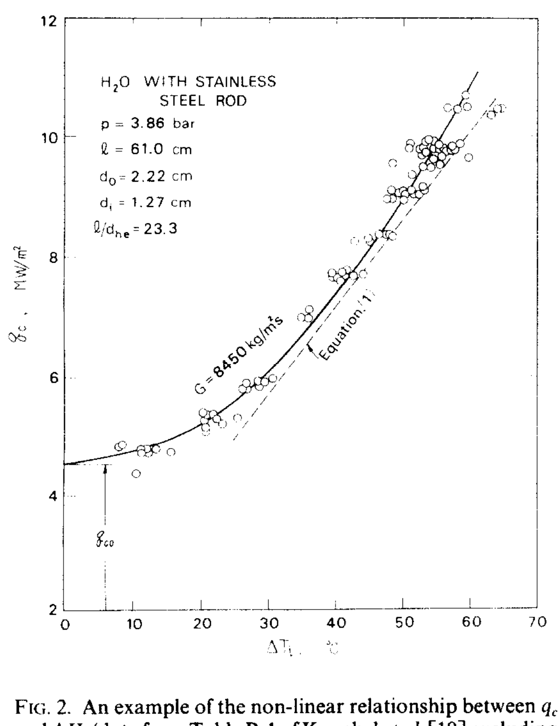

FIG. 2. An example of the non-linear relationship between q_c and ΔH_i (data from Table B-1 of Knoebel *et al.* [19] excluding the data for heaters bowed or with flaws etc.).

annuli with inside heating as follows (cf. [5]):

$$\frac{l}{d_{he}} = \frac{l}{d_i} \cdot \frac{1}{(d_0/d_i)^2 - 1}. \tag{3}$$

Therefore, the method (i) applies to the relation of q_c vs ΔH_i thus obtained.

(iii) Data-sources [8, 10, 38] present data in the form of (ii), but the data are concerned with the uniform heat flux experiment with mixed-inlet-condition (that is, $\Delta H_i < 0$ and $\chi_{in} > 0$). In this case, if the imaginary length l, determined as $l = l'/[1 - (\chi_{in}/\chi_{ex})]$ for the actual length l' used in the experiment, is assumed, the mixed-inlet-condition of $\Delta H_i < 0$ can be formally transformed to that of $\Delta H_i = 0$. Then, according to the author's study [3] of CHF in tubes, the experimental data of CHF for $\Delta H_i < 0$ can be approximately correlated with the imaginary length l mentioned above if exit quality is in the vicinity of unity. Therefore, taking this fact into consideration in the present paper too, 5 data (Run No. 691–695) with $\chi_{ex} > 0.75$ are adopted from Table II of [8], and 13 data (Run No. 2582–2588 and 2599–2604) with $\chi_{ex} > 0.75$ are adopted from Table 2 of [10], but no data are adopted from [37] because all data are of $\chi_{ex} < 0.75$.

(iv) Data-sources [22–24] give the data for independent sets of G, ΔH_i and q_c. Therefore, q_{co} is estimated, through empirical equations (14) and (16) of the preceding paper [5], from the data at $\Delta T_i = 10°C$, for which $\Delta H_i/H_{fg}$ is restricted to small values so that serious error cannot arise for the estimation of q_{co}.

2.2. *Note on the data*

[11] reports two groups of experiments carried out at atmospheric pressure and at 59.9 bar respectively with different apparatus, and the data at atmospheric pressure show quite irregular natures, presumably due to the lack of throttling measures to prevent pulsation flows, so that only the data at 59.9 bar are employed. For the experiment of [17], the rod was heated indirectly with a coiled ribbon electric heater set up in the rod, accordingly there is the possibility of some error not only in the uniformity of heat flux distribution but also in the axial length of heated surface of rod. As for experiments reported in [19] for heavy water and aluminum rods, no data were obtained for CHF in the vicinity of $\Delta T_i = 0$ so that q_{co} cannot be determined, and consequently only the data for light water on a stainless steel rod such as exemplified in Fig. 2 are employed. Experimental data of [21] are given with very small figures so that there is the possibility of low accuracies for q_{co} derived from these data. The data for sodium presented in [31] show a considerable scattering, and the data obtained at the pressure of 0.15 bar for the flow rate of $0.0567\,kg\,s^{-1}$ alone are employed in this study because of comparatively good order. The data of CHF in annuli with inside heating given in [38] cannot be utilized because of lacking the data of mass velocity G.

Table 1. Summary of the collected data of q_{co}

Source	Fluid	l (cm)	d_o (cm)	d_i (cm)	l/d_{he}	$(\rho_v/\rho_l) \times 10^2$	$\sigma\rho_l/G^2 l$	No. of data
G.E. [6]	Water	274	2.22	0.952	64.8	4.84	8.93×10^{-7}–8.04×10^{-6}	4
Blackford–Matzner [7]	Water	107	4.43	3.49	50.0	4.84	1.78×10^{-6}–1.24×10^{-5}	4
Bennett *et al.* [8]	Water	471–649	1.42	0.952	402–554	2.13	7.24×10^{-6}–9.96×10^{-6}	5
Janssen–Kervinen [9]	Water	91.4–177	2.22–2.54	0.952–1.27	24.0–42.0	2.61–7.60	2.95×10^{-7}–2.00×10^{-5}	3
Bennett *et al.* [10]	Water	459–884	1.58	0.952	271–522	2.13–4.84	3.85×10^{-6}–6.61×10^{-6}	13
JSME [11]	Water	30.0	1.90	1.00	11.5	4.05	2.05×10^{-6}–3.28×10^{-5}	4
Barnett [12, 13]	Water	73.6–274	1.40–10.1	0.952–9.64	18.4–287	2.61–8.04	1.97×10^{-7}–2.25×10^{-4}	82
Moeck *et al.* [14]	Water	188	7.95–10.1	7.63–9.64	172–287	4.84	4.07×10^{-7}–1.46×10^{-5}	20
Barnett [15]	Water	182–457	2.09–2.67	1.48–1.54	59.0–387	4.84	1.71×10^{-7}–1.51×10^{-5}	11
Little [16]	Water	365–457	2.09	1.58	310–387	3.39–4.84	1.60×10^{-7}–2.46×10^{-6}	40
Moeck [17]	Water	131	2.37	1.97	146	2.11–4.84	5.27×10^{-6}–9.07×10^{-6}	2
Tolubinskiy *et al.* [18]	Water	22.0	1.30	0.500	7.64–11.5	10.3	4.50×10^{-4}–6.75×10^{-4}	2
Knoebel *et al.* [19]	Water	61.0	2.22	1.27	23.3	0.123–0.224	4.59×10^{-7}–1.12×10^{-6}	3
Tolubinskiy *et al.* [20]	Water	10.0	1.30	1.00	14.5	16.0	1.23×10^{-4}	1
Tolubinskiy *et al.* [21]	Water	10.0–100	1.30	0.900	10.2–102	16.0	3.07×10^{-6}–3.07×10^{-5}	7
Andersen *et al.* [22]	Water	350	2.72	1.70	132	4.94	1.55×10^{-6}–9.74×10^{-6}	10
Jensen–Manov [23]	Water	350	2.60	1.70	154	4.84	1.85×10^{-6}–1.01×10^{-5}	5
Becker–Letzter [24]	Water	300	2.13	1.20	116	1.83–4.94	1.90×10^{-6}–3.04×10^{-5}	5
Mortimore–Beus [25]	Water	213	1.27	0.770	161	6.16–13.5	2.61×10^{-7}–4.33×10^{-5}	12
Stevens *et al.* [26]	R-12	365	2.09	1.58	310	3.60–4.82	4.22×10^{-7}–3.31×10^{-6}	8
Ahmad–Groeneveld [27]	R-12	182	2.22	1.04–1.39	49.4–85.5	4.82–8.49	2.67×10^{-7}–7.07×10^{-4}	48
Shiralkar [28]	R-114	183	2.22	1.43	90.3–180	4.81	4.36×10^{-6}–8.72×10^{-6}	2
Andrews *et al.* [29]	Acetone	7.62	2.09	0.604	1.15	0.290	3.13×10^{-5}	1
Andrews *et al.* [29]	Toluene	7.62	2.09	0.604	1.15	0.385	2.90×10^{-5}	1
Sterman *et al.* [30]	MIPB†	11.0	1.60	1.00	7.05	1.03	2.50×10^{-6}–1.60×10^{-4}	4
Noyes *et al.* [31]	Sodium	68.6	1.27	0.635	36.0	0.00580–0.0211	4.22×10^{-4}–7.64×10^{-4}	4
								Total 301

† Monoisopropylbiphenyl.

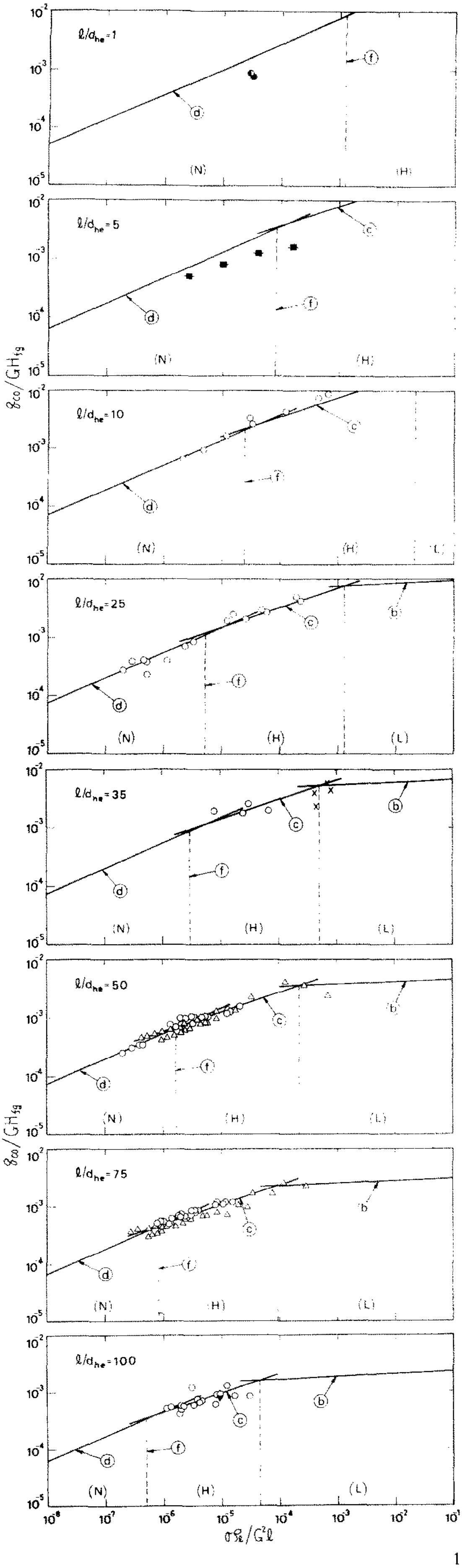
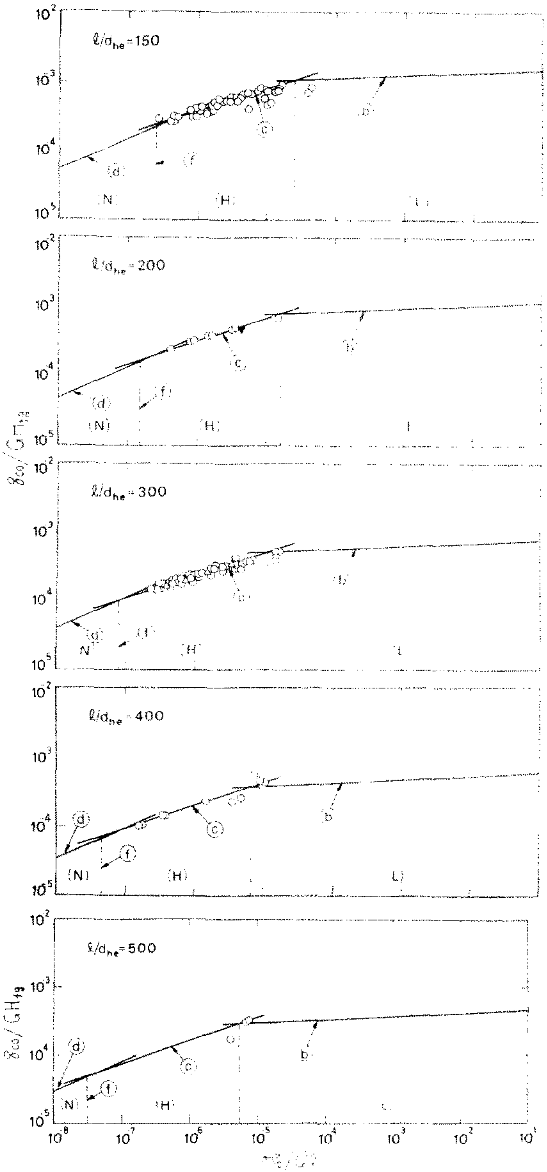

FIG. 3. Generalized graphic representation of q_{co} data. (L): L-regime, (H): H-regime, (N): N-regime, (b): equation (4), (c): equation (5) with $\rho_v/\rho_l = 0.048$, (d): equation (6) with $\rho_v/\rho_l = 0.048$, (f): equation (7).

3. GRAPHIC REPRESENTATION OF q_{co} DATA

3.1. *Representation of* q_{co} *data*

All the experimental data of q_{co} collected in Section 2 are listed in Table 1 along with the kind of test fluid, the range of experimental conditions, and the number of collected data, where it should be noted that physical properties estimated by the method of [35, 36] are used for monoisopropylbiphenyl (MIPB) alone. Then, assuming the possibility of correlating the data of q_{co} with four dimensionless groups of q_{co}/GH_{fg}, ρ_v/ρ_l, $\sigma\rho_l/G^2l$, and l/d_{he}, 13 graphs are prepared for distinct

Table 2. Symbols used to specify the fluids in Fig. 3

Ref. No.	Fluid	Symbol	Ref. No.	Fluid	Symbol
6–25	Water	○	29	Toluene	◑
26, 27	R-12	△	30	MIPB	-■-
28	R-114	▼	31	Sodium	×
29	Acetone	●			

values of l/d_{he} as shown in Fig. 3 and the data of q_{co}/GH_{fg} classified to each graph depending on l/d_{he} are plotted against $\sigma\rho_l/G^2l$ (see Tables 3 and 4 for the division of data by l/d_{he} to each graph and see Section 3.3 for the treatment of the effect of ρ_v/ρ_l). Data symbols shown in Table 2 are used in Fig. 3 to discriminate the kind of fluid.

3.2. *Representation of the author's correlation equations*

Based on the results of the author's study [5], the characteristic regimes L, H and N (cf. [1] for the origin of these names), the correlation lines (b)–(d), and the boundary (f) between H- and N-regime are shown in Fig. 3 applying the following equations:

L-regime,

$$\text{(b)}: \quad \frac{q_{co}}{GH_{fg}} = 0.25\left(\frac{\sigma\rho_l}{G^2l}\right)^{0.043}\frac{1}{l/d_{he}} \tag{4}$$

H- and N-regime,

$$\text{(c)}: \quad \frac{q_{co}}{GH_{fg}} = 0.12\left(\frac{\rho_v}{\rho_l}\right)^{0.133} \times \left(\frac{\sigma\rho_l}{G^2l}\right)^{1/3}\frac{1}{1+0.0081\,l/d_{he}} \tag{5}$$

where $\rho_v/\rho_l = 0.048$ for (c) in Fig. 3.

$$\text{(d)}: \quad \frac{q_{co}}{GH_{fg}} = 0.22\left(\frac{\rho_v}{\rho_l}\right)^{0.133} \times \left(\frac{\sigma\rho_l}{G^2l}\right)^{0.433}\frac{(l/d_{he})^{0.171}}{1+0.0081\,l/d_{he}} \tag{6}$$

where $\rho_v/\rho_l = 0.048$ for (d) in Fig. 3.

Boundary between H- and N-regime,

$$\text{(f)}: \quad \frac{\sigma\rho_l}{G^2l} = \left(\frac{0.0206}{l/d_{he}}\right)^{1.71}. \tag{7}$$

Among the above equations, equation (4) for L-regime is independent of ρ_v/ρ_l, it can be represented by a line (b) in each graph of Fig. 3. On the other hand, equations (5) and (6) for H- and N-regime are subject to the influence of ρ_v/ρ_l, so that the prediction of these equations is given by lines (c) and (d) in Fig. 3 only for the case of $\rho_v/\rho_l = 0.048$, which corresponds to the density ratio of saturated steam and water at 68.5 bar.

3.3. *Effects of ρ_v/ρ_l*

Figure 3 shows that almost all the data points of q_{co} collected in this paper distribute within H- and N-regime. According to equations (5) and (6), the effect of ρ_v/ρ_l on CHF in H- and N-regime may be presumed to be in the mere degree of $(\rho_v/\rho_l)^{0.133}$. Therefore, the data of q_{co} listed in Table 1 are divided into two groups of Tables 3 and 4 depending on the magnitude of ρ_v/ρ_l. As for the data listed in Table 3 with the range of ρ_v/ρ_l between 0.0103 and 0.160, ρ_v/ρ_l is not far apart from 0.048 so that experimental data of q_{co} have been plotted in Fig. 3 without any artificial modification of data. However, as for 9 data listed in Table 4 with the

Table 3. Experimental range of l/d_{he} and ρ_v/ρ_l for the data of Fig. 3, excluding the data of Table 4

Nominal l/d_{he}	$\frac{l}{d_{he}}$	$\frac{\rho_v}{\rho_l} \times 10^2$	Ref. No.
5	7.05	1.03	30
10	7.64–14.5	4.05–16.0	11, 18, 20, 21
25	18.4–26.8	4.84–16.0	9, 12, 21
35	33.8–40.9	4.84–16.0	12, 21
50	42.0–59.0	2.61–8.49	7, 9, 12, 13, 15, 27
75	64.6–85.5	4.82–8.49	7, 12, 27
100	90.3–116	1.83–16.0	12, 13, 21, 28
150	123–172	4.84–13.5	12, 14, 15, 17, 22, 23, 25
200	173–180	4.84	12, 14, 28
300	283–348	2.13–4.84	10, 12, 14, 16, 26
400	316–443	2.13–4.84	6, 8, 10, 15, 16
500	509–553	2.13	8, 10

Table 4. Data with comparatively low values of ρ_v/ρ_l in Fig. 3

Nominal l/d_{he}	$\frac{l}{d_{he}}$	$\frac{\rho_v}{\rho_l} \times 10^2$	No. of data	Ref. No.
1	1.15	0.290–0.385	2	[29]
25	23.3	0.123–0.224	3	[19]
35	36.0	0.00580–0.0211	4	[31]
			Total 9	

range of ρ_v/ρ_l between 0.0000580 and 0.00385, ρ_v/ρ_l is remarkably lower than 0.048, so that the correction of multiplying $[0.048/(\rho_v/\rho_l)]^{0.133}$ to q_{co}/GH_{fg} has been made to be plotted in Fig. 3.

4. DISCUSSION OF THE RESULT OF FIG. 3 WITH CONCLUDING REMARKS

Dealing with CHF of forced convection boiling in internally and uniformly heated annuli with zero inlet subcooling, a graphical representation of 301 data points listed in Table 1 is made to give the result of Fig. 3. Examination of Fig. 3 breeds the following remarks.

(i) It is of interest to note that a number of q_{co} data obtained from various independent sources [6–31] indicate such a regular nature as shown in Fig. 3 for a wide range of l/d_{he}. In addition, these data show a fairly good agreement with the author's correlation equation (5) and (6) in the range of l/d_{he} = 10 to 500, but deviation seems to appear when l/d_{he} decreases to the degree of 1–5. On this point, it may not be useless to note that when l/d_{he} is extremely small, boiling is close to that on a heated rod placed in a uniform liquid flow rather than in an annular channel.

(ii) Most data in the range of l/d_{he} = 10–500 are those of water, and the other test fluids are limited to R-12 (58 data), R-114 (only 2 data) and sodium (only 4 data). Therefore, further experiments should be made in the future with various fluids other than water.

(iii) It is noted that there are almost no data in L-regime except the vicinity of the boundary between L- and H-regime in Fig. 3, and the reason why data lacks for L-regime is unknown. Such being the case, the correlation equation (4) for L-regime must be regarded as a tentative equation at present.

(iv) In cases of l/d_{he} = 50 and 75 in Fig. 3, a statistical trend is observed that the data of R-12 appear slightly lower than those of water in H- and N-regime.

(v) Critical heat flux in HP-regime, such as found for forced convection boiling in tubes or in annuli with outside heating [1–5], should be studied for internally heated annuli too.

Acknowledgements—The Ministry of Education, Science and Culture is acknowledged for the financial support to this study under Grant in Aid of Special Project Research No. 411002 (1979).

REFERENCES

1. Y. Katto, A generalized correlation of critical heat flux for the forced convection boiling in vertical uniformly heated tubes, *Int. J. Heat Mass Transfer* **21**, 1527–1542 (1978).
2. Y. Katto, A generalized correlation of critical heat flux for the forced convection boiling in vertical uniformly heated tubes—a supplementary report, *Int. J. Heat Mass Transfer* **22**, 783–794 (1979).
3. Y. Katto, An analysis of the effect of inlet subcooling on critical heat flux of forced convection boiling in vertical uniformly heated tubes, *Int. J. Heat Mass Transfer* **22**, 1567–1575 (1979).
4. Y. Katto, General features of CHF of forced convection boiling in uniformly heated vertical tubes with zero inlet subcooling, *Int. J. Heat Mass Transfer* **23**, 493–504 (1980).
5. Y. Katto, Generalized correlations of critical heat flux for the forced convection boiling in vertical uniformly heated annuli, *Int. J. Heat Mass Transfer* **22**, 575–584 (1979).
6. Fuel cycle program. A boiling water reactor research and development program. Fourth Quarterly Report, April 1961–June 1961, GEAP-3781 (1961). As quoted in [8].
7. D. Blackford and B. Matzner, Monthly Progress Report Task X, Columbia University Engineering Research Laboratories, New York. MPR-X-8-61 (1961). As quoted in [8].
8. A. W. Bennett, J. G. Collier and P. M. C. Lacey, Heat transfer to mixtures of high pressure steam and water in annulus. Part III: The effect of system pressure on the burn-out heat flux for an internally heated unit, UKAEA. AERE-R 3934 (1963).
9. E. Janssen and J. A. Kervinen, Burnout conditions for single rod in annular geometry, water at 600 to 1400 psia, GEAP-3899 (1963).
10. A. W. Bennett, H. A. Kearsey and R. K. F. Keeys, Heat transfer to mixtures of high pressure steam and water in an annulus. Part VI. A preliminary study of heat transfer coefficient and heated surface temperature at high steam qualities, UKAEA, AERE-R 4352 (1964).
11. 1965 Contract Research for Peaceful Utilization of Atomic Power, Study on Burnout Mechanism, 15 June 1967 Report (in Japanese), pp. 160–161, JSME, Tokyo (1967).
12. P. G. Barnett, A correlation of burnout data for uniformly heated annuli and its use for predicting burnout in uniformly heated rod bundles, UKAEA. Table 4 of AEEW-R 463 (1966).
13. P. G. Barnett, A correlation of burnout data for uniformly heated annuli and its use for predicting burnout in uniformly heated rod bundles, UKAEA, Figs. 1, 2 and 3 of AEEW-R 463 (1966).
14. E. O. Moeck, B. Matzner, J. E. Casterline and G. K. Yuill, Critical heat fluxes in internally heated annuli of large diameter cooled by boiling water at 1000 psia, in *Proceedings of the 3rd International Heat Transfer Conference*, Vol. III, pp. 86–97. A.I.Ch.E., New York (1966).
15. P. G. Barnett, A comparison of the accuracy of some correlations for annuli and rod bundles, UKAEA, AEEW-R 558 (1968).
16. R. B. Little, Dryout tests on an internally heated annulus with variation of axial heat flux distribution, UKAEA, AEEW-R 578 (1970).
17. E. O. Moeck, Annular-dispersed two-phase flow and critical heat flux, Atomic Energy of Canada Ltd., AECL-3656 (1970).
18. V. I. Tolubinskiy, A. K. Litoshenko and V. L. Shevtsov, Critical heat flux densities in internally-heated annuli, *Heat Transfer—Soviet Res.* **2**(6), 183–186 (1970).
19. D. K. Knoebel, S. D. Harris, B. Crain, Jr. and R. M. Biderman, Forced-convection subcooled critical heat flux, D_2O and H_2O cooled with aluminum and stainless steel heaters, Du Pont Savannah River Lab., DP-1306 (1973).
20. V. I. Tolubinskiy, A. K. Litoshenko and V. L. Shevtsov, Effect of curvature on the critical heat flux density in forced-convection flow, *Heat Transfer—Soviet Res.* **5**(1).

21–25 (1973).
21. V. I. Tolubinskiy, A. L. Litoshenko, V. L. Shevtsov, Ye. D. Domashev and G. Ye. Struchenko, Heat transfer crisis at the inward surface of annuli heated from both sides, *Heat Transfer—Soviet Res.* **5**(3), 93–96 (1973).
22. P. S. Andersen, A. Jensen, G. Mannov and A. Olsen, Burn-out, circumferential film flow distributions and pressure drop for an eccentric annulus with heated rod, *Int. J. Multiphase Flow* **1**, 585–600 (1974).
23. A. Jensen and G. Mannov, Measurements of burnout film thickness and pressure drop in a concentric annulus 3500 × 26 × 17 mm with heated rod and tube, European Two-Phase Flow Group Meeting, Harwell (1974). As quoted in [32].
24. K. M. Becker and A. Letzter, Burnout measurements for flow of water in an annulus with two-sided heating, European Two-Phase Flow Group Meeting, Haifa (1975). As quoted in [33].
25. E. P. Mortimore and S. G. Beus, Critical heat flux experiments with a local hot patch in an internally heated annulus, WAPD-TM-1419 (1979).
26. G. F. Stevens, R. W. Wood and J. Pryzbyski, An investigation into the effect of a cosine axial heat flux distribution on burnout in a 12-ft long annulus using Freon-12, UKAEA, AEEW-R 609 (1968).
27. S. Y. Ahmad and D. C. Groeneveld, Fluid modelling of critical heat flux in uniformly heated annuli, International Symposium on Two-Phase Systems, Haifa (1971), Paper 1–8; or AECL-4070 (1972).
28. B. S. Shiralkar, Analysis of non-uniform flux CHF data in simple geometries, NEDM-13279 (1972). As quoted in [34].
29. D. G. Andrews, F. C. Hooper and P. Butt, Velocity, subcooling and surface effects in the departure from nucleate boiling of organic binaries, *Can. J. Chem. Engng* **46**, 194–199 (1968).
30. L. Sterman, A. Abramov and G. Checheta, Investigation of boiling crisis at forced motion of high temperature organic heat carriers and mixtures, in *Cocurrent Gas–Liquid Flow*, pp. 455–470. Plenum Press, New York (1969).
31. R. C. Noyes and H. Lurie, Boiling sodium heat transfer, in *Proceedings of the 3rd Int. Heat Transfer Conference*, Vol. V, pp. 92–100. A.I.Ch.E., New York (1966).
32. V. Marinelli, Critical heat flux, a review of recent publications, *Nucl. Technol.* **34**, 135–171 (1977).
33. J. Würtz, An experimental and theoretical investigation of annular steam–water flow in tubes and annuli at 30 to 90 bar, Risø National Lab., Risø Report No. 372 (1978).
34. R. T. Lahey and J. M. Gonzalez, The effect of non-uniform axial heat flux on critical power, in *Inst. Mech. Engrs Conference Publications 1977–1978*, pp. 193–197 (1977).
35. T. C. Core and K. Sato, Determination of burnout limits of polyphenyl coolants, AEC Research and Development Report, IDO-28007 (1958).
36. W. R. Gambill, How to estimate engineering properties, *Chem. Engng* 261–266 (December 1957), 195–202 (19 October, 1959), 146–150 (7 April, 1958), 263–268 (July 1957).
37. A. W. Bennett, J. G. Collier and P. M. C. Lacey, Heat transfer to mixtures of high pressure steam and water in an annulus. Part II. The effect of steam quality and mass velocity in the 'burnout' heat flux for an internally heated unit at 1000 psia, UKAEA, AERE-R 3804 (1961).
38. K. M. Becker and G. Hernborg, Measurements of burnout conditions for flow of boiling water in a vertical annulus, *J. Heat Transfer* **86**, 393–407 (1964).

CONFIGURATIONS GENERALES DE LA CONVECTION FORCEE AVEC EBULLITION AU FLUX CRITIQUE, DANS UN ESPACE ANNULAIRE VERTICAL AUTOUR D'UNE BARRE CHAUFFEE UNIFORMEMENT ET AVEC UN SOUS-REFROIDISSEMENT NUL A L'ENTREE

Résumé—On emploie une méthode graphique pour donner une vue d'ensemble des données existantes pour le flux de chaleur critique (CHF) dans des espaces annulaires, verticaux, uniformément chauffés intérieurement et avec un sous-refroidissement nul à l'entrée. 301 données sont tirées de 25 sources et ils concernent 7 fluides différents (eau, R-12, R-114, acétone, toluène, monoisopropylbiphényl et sodium), des longueurs chauffées de 0,0762–8,84 m, des diamètres externes de barre chauffée entre 0,005 et 0,0964 m, des diamètres internes de tube enveloppant entre 0,0127 et 0,101 m, et des rapports vapeur/liquide depuis 0,000058 jusqu'à 0,160.

ALLGEMEINE MERKMALE DER KRITISCHEN WÄRMESTROMDICHTE (KWD) BEIM STRÖMUNGSSIEDEN IN SENKRECHTEN KONZENTRISCHEN RINGSPALTEN MIT GLEICHMÄSSIG BEHEIZTEM STAB OHNE UNTERKÜHLUNG AM EINTRITT

Zusammenfassung — Um einen allgemeinen Überblick über die vorhandenen Daten für die kritische Wärmestromdichte in von innen gleichmäßig beheizten senkrechten Ringspalten ohne Unterkühlung am Eintritt zu erhalten, wurde eine grafische Methode angewandt. Aus 25 Quellen wurden 301 Angaben zu diesem Zweck zusammengetragen. Diese umfassen: sieben verschiedene Fluide (Wasser, R12, R114, Aceton, Toluen, Monoisopropylbiphenyl und Natrium), axiale Längen des beheizten Stabes von 0,0762 bis 8,84 m, äußere Durchmesser des beheizten Stabes von 0,005 bis 0,0964 m, innere Durchmesser des äußeren Mantelrohres von 0,0127 bis 0,101 m und Dampf/Flüssigkeits-Verhältnisse von 0,000058 bis 0,16.

О КРИТИЧЕСКОМ ТЕПЛОВОМ ПОТОКЕ ПРИ КИПЕНИИ В УСЛОВИЯХ ВЫНУЖДЕННОЙ КОНВЕКЦИИ В ВЕРТИКАЛЬНЫХ КОНЦЕНТРИЧЕСКИХ КАНАЛАХ С РАВНОМЕРНО НАГРЕВАЕМЫМ СЕРДЕЧНИКОМ БЕЗ НЕДОГРЕВА НА ВХОДЕ

Аннотация Используя графический метод, проведен обзор имеющихся данных по критическому тепловому потоку в равномерно нагреваемых изнутри кольцевых каналах при отсутствии недогрева на входе. С этой целью была взята 301 точка из 25 публикаций для 7 жидкостей (вода, R-12, R-114, ацетон, толуол, моноизопропил-бифенил, натрий). Длина нагреваемого сердечника по оси составляла 0,0762 8,84 м, наружный диаметр сердечника изменялся от 0,00500 до 0,0964 м, внутренний диаметр ненагреваемой трубы изменялся от 0,0127 до 0,101 м, а отношение содержаний пара и жидкости изменялось в пределах от 0,0000580 до 0,160.